Nanoscale

Accepted Manuscript

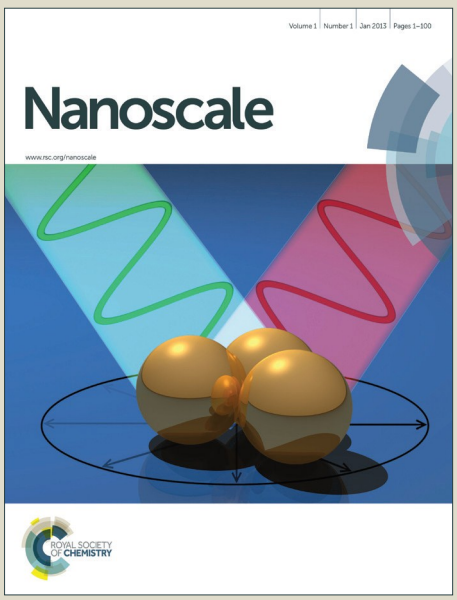

ROYAL SOCIETY OF CHEMISTRY

www.rsc.org/nanoscale

Nanoscale

ARTICLE

Near Infrared Light-Actuated Gold Nanorods with Cisplatin-Polypeptide Wrapping for Targeted Therapy of Triple Negative Breast Cancer

Received 00th January 20xx,
Accepted 00th January 20xx

DOI: 10.1039/x0xx00000x

www.rsc.org/

Bing Feng[a,‡], Zhiai Xu[b,‡], Fangyuan Zhou[a], Haijun Yu[a,*], Qianqian Sun[c], Dangge Wang[a], Zhaohui Tang[c], Haiyang Yu[c], Qi Yin[a], Zhiwen Zhang[a], Yaping Li[a,*]

Despite considerable progress has been made in breast cancer therapy, the complete eradication of highly aggrevasive triple negative breast cancer (TNBC) remains a notable challenge today. We herein report on the fabrication of novel gold nanorods (GNRs) with covalent cisplatin-polypeptide wrapping and folic acid (FA) conjugation (denoted as FA-GNR@Pt) for targeted photothermal (PT) and chemotherapy of TNBC. The FA-GNR@Pt hybrid nanoparticles are designed to integrate the photothermal conversion property of GNRs, the superior biocompatibility of polypeptide poly(L-glutamic acid) (PGA), the chemotoxicity of cisplatin, and the tumor targeting ability of FA into one single nanoplatform. In combination with localized near infrared (NIR) laser illumination, the resulting FA-GNR@Pt hybrid nanoparticles are able to significantly inhibit the growth of the TNBC tumor when administrated systemically. In particular, they can extensively suppress the dissemination of TNBC cells from the primary tumor to the lung by eliminating the peripheral tumor blood vessels. Collectively, our studies demonstrate that combined and PT chemotherapy using cisplatin-loaded GNRs with FA conjugation might imply a promising strategy for targeted treatment of TNBC.

1. Introduction

Breast cancer is one of the leading cancer types worldwide.[1,2] Triple-negative breast cancer (TNBC) with low level or without expression of the estrogen receptors, progesterone receptors, and Her2/Neu, is the most aggressive subtype of breast cancer.[3] Mono or combined chemotherapy using cytotoxic drugs including cisplatin, paclitaxel or doxorubicin is currently the standard approach approved for clinical treatment of TNBC.[4] Notably, no alternative options are available yet for TNBC therapy after initial responsive to chemotherapy and subsequent development of resistance.[5-7] Moreover, accumulated evidence suggests that chemotherapy tend to elicit tumor invasion and metastasis as a mechanism of cancer cells defence against the cytotoxic stress.[8-11] The progression and metastasis of the solid tumors including TNBC are highly associated with the process of angiogenesis.[12] The new blood vessels forming towards and inside the primary tumor can not only supply nutrient and oxygen for tumor growth, but also facilitate extravasation of the cancer cells from the primary site.[13] These findings had led to the extensive investigation of antiangiogenic drugs to reduce the mortality and morbidity of invasive or metastatic breast cancer. However, angiogenesis therapy was unable to or only marginally improves the overall survival rate due to the occurrence of resistance, the poor pharmacokinetic and low tumor specificity of small molecular drugs.[14,15]

In recent years, near infrared (NIR) light-mediated photothermal (PT) therapy has gained increasing attention for cancer treatment due to its minimal invasiveness and highly spatial selectivity. PT therapy can cause apoptosis or necrosis of the cancer cells and suppress tumor growth by inducing localized hyperthermia effect.[16-18] Combinational PT and chemotherapy has displayed promising potential to improve the therapeutic efficacy against various solid tumors,[19-21] yet few studies has demonstrated successful treatment of TNBC.[22] Among the photoabsorbents employed for PT therapy, gold nanorods (GNRs) were most intensively exploited due to their tunable longitudinal sur-

[a] State key Laboratory of Drug Research & Center of Pharmaceutics, Shanghai Institute of Materia Medica, Chinese Academy of Sciences, Shanghai 201203, China; E-mails: hjyu@simm.ac.cn; ypli@simm.ac.cn
[b] Department of Chemistry, East China Normal University, Shanghai 200241, China;
[c] Key Laboratory of Polymer Ecomaterials, Changchun Institute of Applied Chemistry, Chinese Academy of Sciences, Changchun 130022, China
‡ These two authors contributed euqlly to this study.

§Electronic Supplementary Information (ESI) available: Polymer synthesis, fabrication of cisplatin-loaded GNR (GNR@Pt) nanoparticles, *in vivo* pharmacokinetics and biodistribution of GNR@Pt nanoparticles, *in vitro* and *in vivo* antitumor studies. See DOI: 10.1039/x0xx00000x.

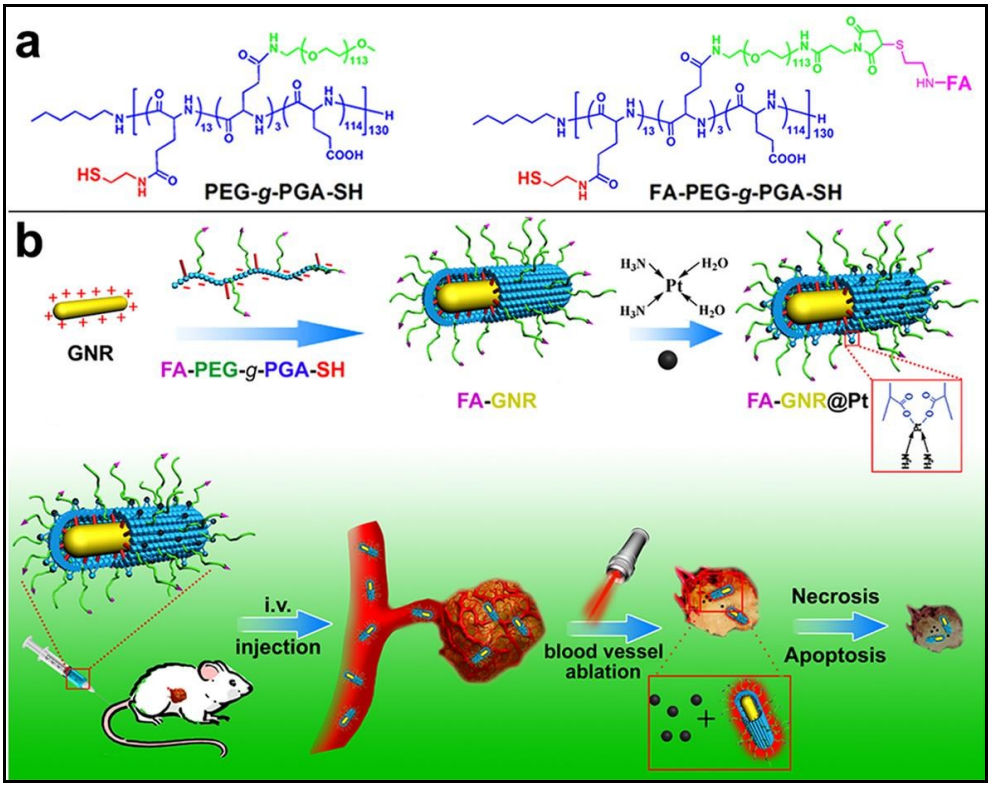

Scheme 1. Characteristics of GNR@Pt nanoparticles. (a) UV-Vis spectrum of CTAB-GNR, GNR-PGA and GNR@Pt nanoparticles; (b) The change of surface charge during PGA wrapping and cisplatin loading; (c) Cisplatin loading ratio and loading efficacy in GNR-PGA nanoparticles determined by ICP-MS; (d) Representative TEM image of GNR@Pt nanoparticles (scale bar 50 nm); (e) Laser intensity-dependent temperature elevation, and (f) The corresponding thermographs of GNR@Pt nanoparticles determined at an Au concentration of 150 μM; (g) Concentration-dependent temperature elevation determined at a laser intensity of 4.0 W/cm^2, and (h) The corresponding thermographs of GNR@Pt nanoparticles.

plasmon resonance (LSPR) absorbance, and high photothermal conversing efficiency in the near infrared (NIR) region.[16,23] However, the implementation of GNR-mediated PT therapy is hindered with the cytotoxic surfactant cetyl trimethylammonium bromide (CTAB), the latter is a crucial component used for the synthesis of GNRs. Although the cytotoxicity of CTAB-protected GNR (CTAB-GNR) can be minimized by substituting CTAB with thiolated polyethylene glycol (PEG), the biomedical application of PEGylated GNRs suffer from the low functionality of PEG.[25]

To pursuit novel strategy for combating TNBC, we herein developed GNR-based platform with cisplatin-polypeptide wrapping and folic acid (FA) functionalization (namely, FA-GNR@Pt) for targeted PT and chemotherapy of breast cancer. The FA-GNR@Pt nanoparticles were designed to integrate the photothermal property of GNRs, the excellent biocompatibility of the polypeptide poly(L-glutamic acid) (PGA), the superior cytotoxicity of cisplatin (Pt), and the tumor targeting ability of FA into one nanocomposite. The FA-GNR@Pt nanoparticles presented in this study possess several unique advantages. Firstly, GNRs was covalently coated with biodegradable PGA by forming multivalent Au-S bonds between GNRs and thiolated PGA, thus preventing PGA dissociation during cisplatin loading and blood circulation, and highly efficiently removed CTAB moiety and minimized the toxicity of GNRs. Secondly, the carboxyl groups of PGA can be used for loading cisplatin GNRs via formation of metal-polymer complex. The cisplatin payload could be reversely released in tumor site or cancer cells in the presence of chloride ion. Moreover, PEG corona presenting on the outlayer of GNR-PGA nanoparticles can reduce protein absorption and elongate the blood circulation of GNR@Pt nanoparticles. Furthermore, a combination of cisplatin-mediated chemotherapy with GNR-performed PT therapy is of vital importance to prevent tumor relapse and distant metastasis by eliminating both the seeds (i.e. cancer cells) and nutrient line (i.e. tumor-associated blood vessels) for tumor growth and metastasis (**Scheme 1**).

2. Results and Discussion

Fabrication and characterization of FA-GNR@Pt nanoparticles

To prepare the GNR@Pt or FA-GNR@Pt hybrid nanoparticles, thiolated poly(ethylene glycol)-graft-poly(L-glutamic acid) copolymers with and without FA modification (FA-PEG-*g*-PGA-SH or mPEG-*g*-PGA-SH) (Scheme 1a) were synthesized according to the procedures described in the Supplemental Information (see Figure SI 1-7 for synthesis and characterization, respectively). CTAB-GNRs (GNRs) were then covalently coated with mPEG-*g*-PGA-SH copolymer to obtain GNR-PGA through electrostatic interaction and formation of Au-S bonds between GNRs and thiolated PGA. The GNR-PGA prepared at the optimized Au to PGA molar ratio of 7.5 displayed the highest LSPR absorption. The surface charge of GNRs switched accordingly from 27.3±0.3 mV to -25.6±0.7 mV (Figure SI 8a&b). Cisplatin, a cytotoxic drug with wide anticancer spectrum was then loaded on GNR-PGA via

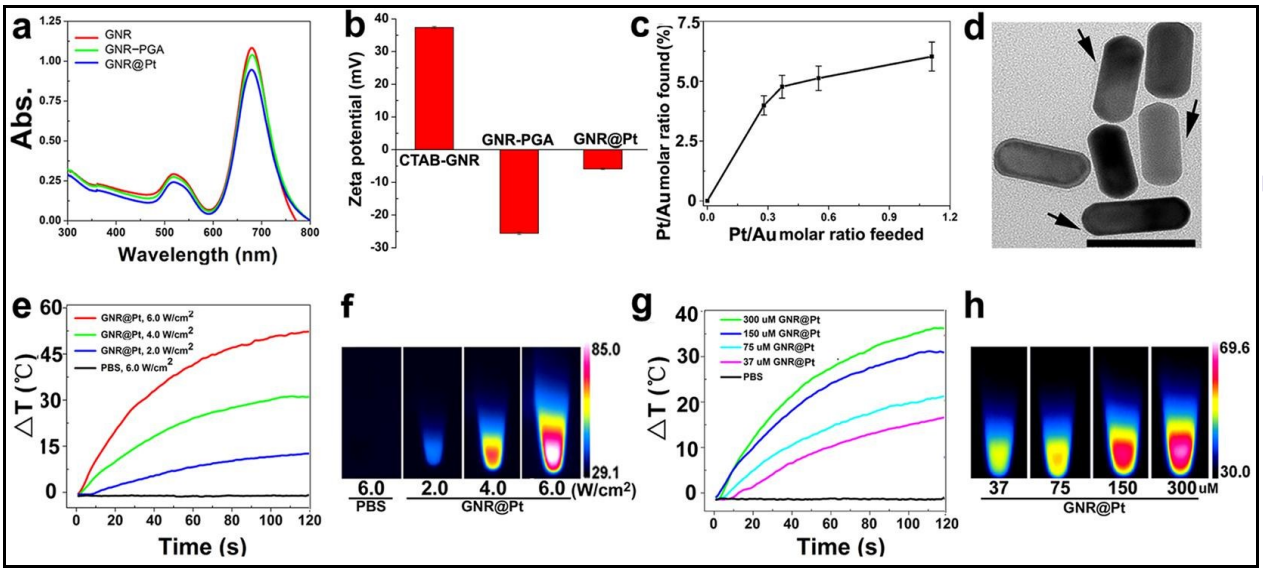

Fig. 1. Characteristics of GNR@Pt nanoparticles. (a) UV-Vis spectrum of CTAB-GNR, GNR-PGA and GNR@Pt nanoparticles; (b) The change of surface charge during PGA wrapping and cisplatin loading; (c) Cisplatin loading ratio and loading efficacy in GNR-PGA nanoparticles determined by ICP-MS; (d) Representative TEM image of GNR@Pt nanoparticles (scale bar 50 nm); (e) Laser intensity-dependent temperature elevation, and (f) The corresponding thermographs of GNR@Pt nanoparticles determined at an Au concentration of 150 μM; (g) Concentration-dependent temperature elevation determined at a laser intensity of 4.0 W/cm^2, and (h) The corresponding thermographs of GNR@Pt nanoparticles.

formation of coordination bonds between the carboxylic groups of PGA and the platinum atom of cisplatin (Scheme 1b).[26,27] A cisplatin to Au loading ratio of 4.8 wt% and a drug loading efficiency of 13.0% were achieved when GNR@Pt nanoparticles were prepared at a cisplatin to Au feeding ratio of 0.37 as determined using inductively coupled plasma mass spectrometry (ICP-MS) measurement (Figure 1c). The LSPR absorbance of GNR-PGA decreased slightly upon cisplatin loading, which might be caused by sample loss during centrifugation (Figure 1a & SI 8). After cisplatin loading, the surface charge of GNR-PGA increased to –4.1±0.2 mV due to consumption of the carboxylic groups during cisplatin complexation (Figure 1b).

The morphology of the resulting GNR@Pt nanoparticles was characterized by transmission electron microscopic (TEM) examination. A thin corona was found on the surface of GNR-PGA and GNR@Pt nanoparticles, confirming the successful coating of GNRs with PGA (Figure 1d&SI 9). The GNR@Pt nanoparticles dispersed as well as parental GNR or GNR-PGA ones, indicating the formation of metal-polymer complex between cisplatin and PGA did not induce aggregation of GNR-PGA nanoparticles. This could be presumably attributed to the formation of the covalent Au-S bonds between PGA and GNRs. The covalent coating strategy can also significantly reduce the cytotoxicity of CTAB-GNR by replacing CTAB with PGA copolymer (Figure SI 10).

The colloidal stability of GNR-PGA and GNR@Pt nanoparticles was evaluated in water, phosphor buffer saline (PBS) or complete fetal bovine serum (FBS) solution, respectively. No decrease of LSPR absorbance was detected in water or FBS solution of GNR@Pt after 7 days storage at room temperature (Figure SI 11&12), implying good colloidal stability of GNR@Pt nanoparticles due to the presence of PGA outer layer and PEG corona. A drug release study showed that around 40% of cisplatin was released from the PGA-GNR nanoparticles after 24 h incubation in 0.9 wt% saline solution due to the ligand exchange reaction between chloride ion and the carboxylic group of PGA (Figure SI 13).[28]

We next examined the photothermal effect of GNR@Pt nanoparticles by measuring NIR laser illumination-induced temperature elevation. As shown in Figure 1e-h, after irradiated with 655 nm laser for 120 s at photo density of 6.0 W/cm^2, GNR@Pt induced significant temperature increase >50 ℃ at a GNR concentration of 150 μM. Moreover, the hyperthermia effect of GNR@Pt could be readily tuned by adjusting the GNR concentration and laser dose. Collectively, all these results suggesting good potential of GNR@Pt nanoparticles for PT therapy application.

To realize tumor targeted PT and chemotherapy of breast cancer, we firstly coated CTAB-GNRs using a mixed solution of FA-PEG-*g*-PGA-SH and Rhodamine B labelled PEG-g-PGA copolymer (RhoB-PEG-*g*-PGA-SH, see Figure SI 14 for synthesis) and then loaded cisplatin on the surface of the resulting FA-GNR-PGA nanoparticles to obtain FA-modified GNR@Pt nanoparticles (FA-GNR@Pt). The latter displayed the similar physio-chemical properties as those of the GNR@Pt ones (data not shown). The internalization of the FA-GNR@Pt nanoparticles was examined in 4T1 TNBC cells using a flow cytometric method. As demonstrated in Figure 2a&b, FA-GNR@Pt-treated 4T1 cells displayed 3.0 and 3.3-fold magnitude higher RhoB fluorescence intensity than the cells incubated with GNR@Pt ones when examined after 2 h and 4 h nanoparticle incubation, respectively. The intracellular fluorescence intensity of FA-GNR@Pt and GNR@Pt incubated cells became comparable when the incubation time was elongated to 12h. Similar trends of intracellular fluorescence intensity change were found by confocal laser scanning microscopic (CLSM) examination (Figure 2c). Both the flow cytometric and CLSM data consistently suggested that FA-modification significantly accelerated the internalization of the GNR@Pt nanoparticles. The cellular uptake data was in good

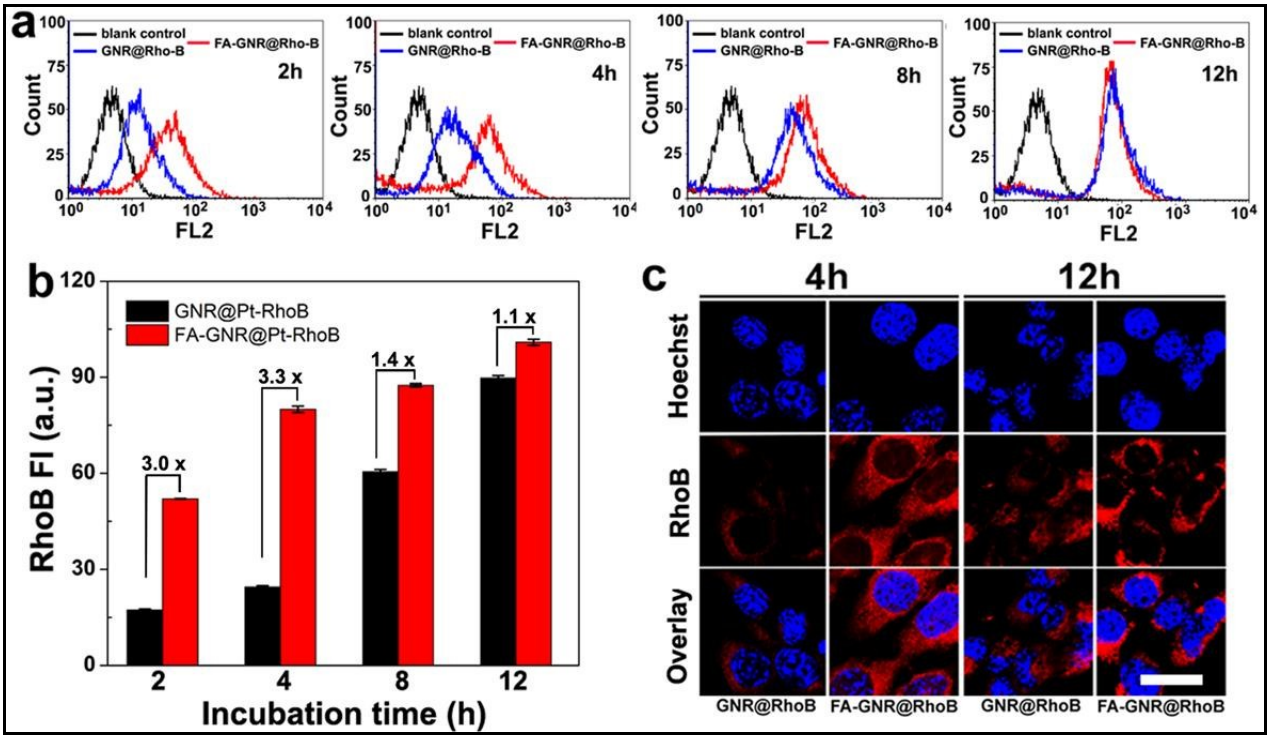

Fig. 2. FA-mediated targeted delivery of GNR@Pt nanoparticles in 4T1 cells. The nanoparticles were covalently labelled with RhoB for fluorescence imaging and flow cytometry measurement. (a) Representative flow cytometric curves of intracellular fluorescence intensity examined at desired time intervals post GNR@Pt-RhoB or FA-GNR@Pt-RhoB incubation; (b) Flow cytometry determined intracellular RhoB fluorescence intensity of 4T1-cells co-incubated with GNR@RhoB or FA-GNR@RhoB nanoparticle for 2h, 4h, 8h or 12h; (c) CLSM images of 4T1 cells co-incubated with GNR@Pt-RhoB or FA-GNR@Pt-RhoB nanoparticle for 4h or 12h (scale bar 50 μm).

agreement with the literature reports and our previous observation that while ligand modification (i.e. epidermal growth factor (EGF) or cyclic RGD) could not increase the total amount of nanoparticles entering the cells, the ligand-receptor interaction strongly accelerates the internalization of nanoparticles.[25,29,30]

The influence of incubation time on the chemotoxicity of FA-GNR@Pt and GNR@Pt nanoparticles was examined using MTT assay since FA modification notably speeded up the internalization ofGNR@Pt nanoparticles. It seems that nanoparticle incubation time significantly affected the cytotoxicity of cisplatin-loaded nanoparticles. Compared with GNR@Pt and cisplatin, FA-GNR@Pt displayed the highest cytotoxicity after 4 h incubation (Figure 3a). This could be most likely explained by the higher intracellular GNR@Pt concentration as revealed by cellular uptake studies. The cell viability decreased over the time, and comparable cytotoxicity was found between FA-GNR@Pt and GNR@Pt nanoparticles after 24 h incubation (Figure 3b).

Given the notable hyperthermia effect of GNR@Pt nanoparticles upon 655 nm laser irradiation, the ability of GNR@Pt and FA-GNR@Pt nanoparticles to ablate tumor cells was further. As shown in Figure 3c&d, GNR-PGA and FA-GNR-PGA nanoparticles both significantly reduced the viability of 4T1 cells upon laser irradiation. For instance, the relative viability of GNR-PGA-treated cells reduced from 0.96 to 0.28 after exposed to655 nm laser for 6 min. The cytotoxicity of GNR-PGA or FA-GNR-PGA nanoparticles increased further by loading cisplatin on the surface. The chemo- and phototoxicity of FA-GNR@Pt nanoparticles was further visualized by live-dead staining assay. 4T1 cells were pre-incubated with FA-GNR@Pt nanoparticles or other formulations at an equal cisplatin concentration of 5.3 μM or Au concentration of 105 μM for 4 h. The cells were then illuminated with 655 nm laser. Afterwards, the cells were stained with a mixed solution of ethidium homodimer-1 (EthD-1), Hoechst 33342 and Calcein AM (AM) to distinguish live (green fluorescence), dead (red fluorescence) and apoptotic cells (blue fluorescence), respectively, as described in our previous study.[31] When treated with cisplatin and illuminated with 655 nm laser, no cells were stained with red or blue fluorescence belonging to EthD-1 or Hoechst, respectively, implying unobvious phototoxicity of cisplatin. In contrast, the cells treated with FA-GNR@Pt and laser illumination were strongly stained with EthD-1 and Hoechst, but not AM, indicating significant DNA damage and loss of the membrane integrity, suggesting an addictive therapeutic effect between cisplatin and FA-conjugated GNRs (Figure 3e).

In Vivo behaviour of FA-GNR@Pt nanoparticles

Cisplatin is a first-line anticancer drug for treatment of various malignant tumors including breast cancer. However, the clinical implementation of cisplatin was hindered by its poor water solubility and low lipophilicity.[26] In this study, FA-PGA-wrapped GNRs were employed as a dual-functional nanocarrier for tumor targeted delivery of cisplatin and photoabsorbent for PT cancer therapy. To testify the efficiency of GNR-PGA for systemic cisplatin delivery, the pharmacokinetic behaviour of FA-GNR@Pt and GNR@Pt nanoparticles was firstly evaluated by quantifying the blood concentration of Au and Pt using ICP-MS measurement. Our data

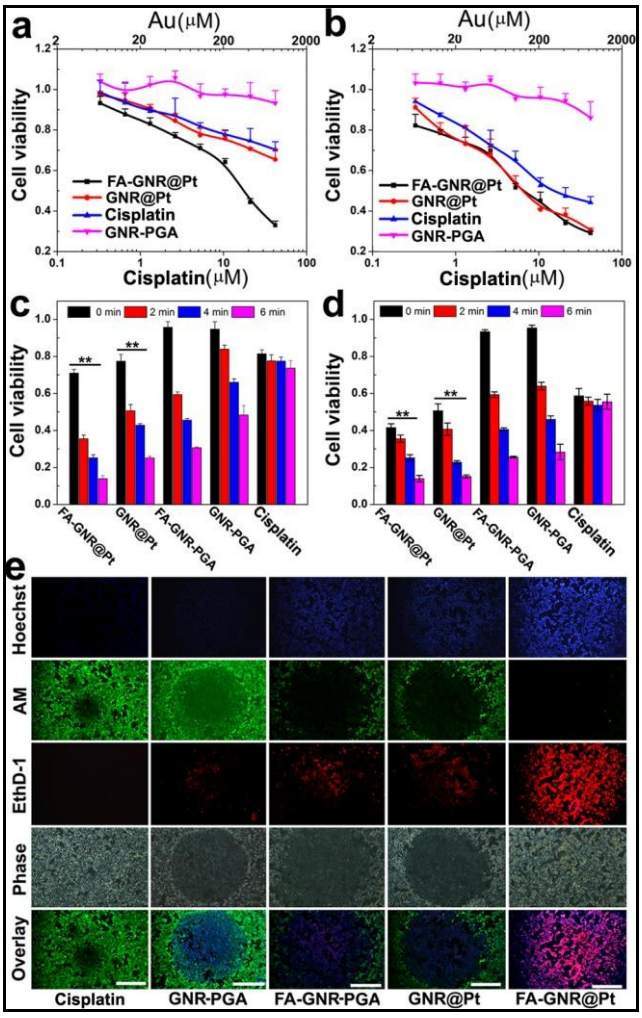

Fig. 3. Cytotoxicity assay of GNR@Pt nanoparticles in 4T1 cells. (a & b) Relative cell viability of 4T1 cells after incubated with FA-GNR@Pt, GNR@Pt, cisplatin or PGA-GNR nanoparticles for (a) 4 h or (b) 24 h; (c &d) Relative viability of 4T1 cells incubated with FA-GNR@Pt, GNR@Pt, cisplatin or PGA-GNR nanoparticles and treated with 655 nm NIR laser irradiation for different time durations (i.e. 2, 4 or 6 min). The cells were pre-incubated with FA-GNR@Pt, GNR@Pt, FA-GNR-PGA, GNR-PGA or cisplatin at cisplatin concentration of 5.3 μM and Au concentration of 105 μM for (c) 4h, or (d) 24h, and then exposed to laser irradiation (laser density of 2.0 W/cm^2); (e) Live-apoptotic-dead staining assay of 4T1 cells treated with GNR@Pt nanoparticles and laser irradiation. The cells were pre-incubated with FA-GNR@Pt, GNR@Pt, FA-GNR-PGA PGA-GNR or cisplatin at equal cisplatin concentration of 5.3 μM and Au concentration of 105 μM for 4 h. The cells were then illuminated with 655 nm laser for 20 min at photo density of 2.0 W/cm^2 (scale bar 400 μm).

showed that GNR@Pt nanoparticles exhibited satisfied blood retention potential over an examination period of 24 h. For instance, around 23.5% and 5.1% of injected dose (ID) of the nanoparticles were retained in blood at 12 h and 24 h post injection (Figure 4a). Using a two compartment model we previously applied to fit the circulation results of polymeric nanoparticles,[20] the elimination half-life ($t_{1/2\beta}$) of GNR@Pt nanoparticles was calculated to be 9.7 h. The significantly increased blood retention of GNR@Pt nanoparticles could be presumably attributed to the stealth effect of PEG corona, which could reduce the non-specific protein binding and avoid GNR aggregation during circulation. The area under the curves (AUC) of cisplatin delivered with FA-GNR@Pt and GNR@Pt nanoparticle was 14.7 and 13.3 mg/L*h, which was 5.1 and 4.6-fold higher tha that of free cisplatin, respectively (Figure 4b). The pharmacokinetic data suggested that the blood circulation of cisplatin was obviously elongated when delivered with GNR-PGA nanocarriers.

The organ distribution of GNRs and cisplatin was examine using ICP-MS measurement. As shown in Figure 4c-d, the tumoural Au and Pt concentration of the FA-GNR@Pt group was 2.1 and 3.(fold magnitude higher than that of the GNR@Pt group respectively, when examined at the 2h time point post nanoparticle administration, which can be most likely attributed to the actively tumor targeting effect of FA-GNR@Pt nanoparticles. In addition to the enhance tumor accumulation of GNRs and cisplatin, it was worth noting th GNR@Pt nanoparticles with or without FA modification preferred t distribute in the liver. For instance, over 30 ID% of GNRs and 6 ID% of cisplatin was found in the liver 2 h post nanopart administration, indicating liver retention with the reticuloendothelial system was the dominant mechanism underlying blood clearanc GNR@Pt nanoparticles.

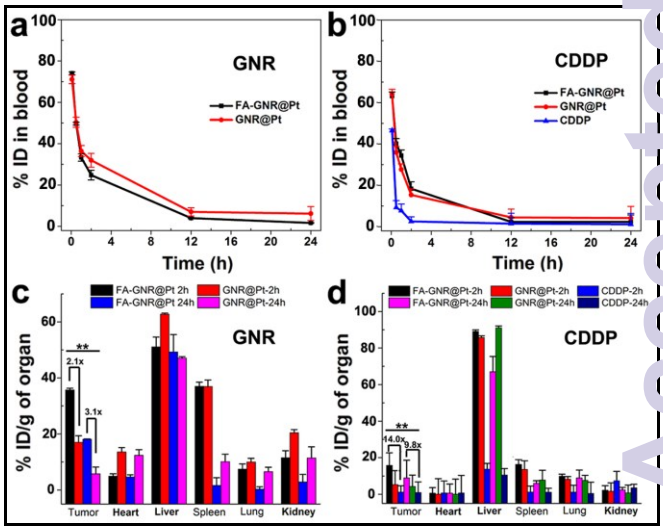

Fig. 4. Pharmacokinetic and biodistribution of intravenously injected FA-GNR@Pt and GNR@Pt nanoparticles in vivo. (a & b) The blood concentration of the hybrid nanoparticles was determined by measuring (a) GNR, and (b) cisplatin concentration, respectively. (c & d) Biodistributio of (c) GNR, and (d) Cisplatin in tumor and major organs (i.e. heart, liver, spleen, lung and kidney) determined at 2 h or 24 h after injection (n = 3).

Hyperthermia effect of GNR@Pt nanoparticles an photothermal tumor ablation *in vivo*

The laser irradiation-induced temperature elevation of the orthotop breast tumor was measured at the desired time intervals (i.e. 0.5h, 1h and 2h) post intravenous administration of the nanoparticles. GNR PGA, GNR@Pt and FA-GNR@Pt nanoparticles all induced significant temperature elevation upon localized laser illumination of the 4T1 tumors. The temperature elevation reached a plateau when examined at 2 h post *i.v.* administration, and a maximal temperature

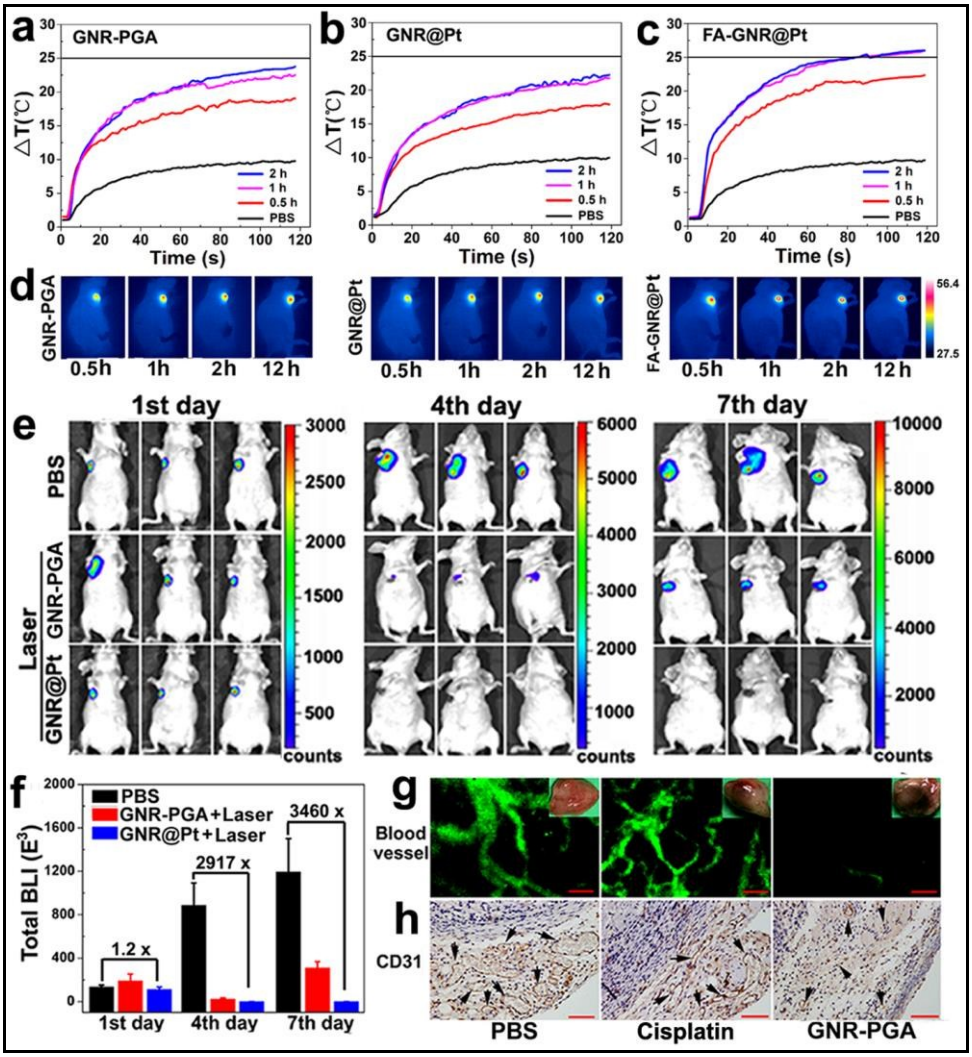

Fig. 5. Hyperthermia effect and photothermal ablation of tumor blood vessels in vivo. (a-d) Laser irradiation temperature elevation in 4T1 tumor-bearing mice injected with (a) GNR-PGA, (b) GNR@Pt, or (c) FA-GNR@Pt nanoparticles. The temperature rise was examined at different time intervals post intravenous injection; (d) The representative thermographs of laser irradiated mice recorded at different time interval post injection; (e) Representative whole-body BLI images of 4T1-Luc tumor-bearing mice taken at the 1st, 4th or 7th day post nanoparticle injection and laser irradiation; (f) The BLI intensity change of 4T1-Luc orthotropic tumors post laser irradiation; (g) Blood perfusion in tumor blood vessels. The tumor-bearing mice were intravenously injected with PBS, cisplatin or GNR-PGA nanoparticles, respectively. The mice were illuminated with 655 nm NIR laser for 2 min at 2 h post injection; (h) Microvessel density (MVD) examination at the 7th day post laser illumination, the blood vessels were stained with CD-31 antibody (scale bar 50 μm).

increase over 20 ℃ was achieved due to time-dependent tumoural accumulation of the nanoparticles (Figure 5a-d).[32]A slight temperature increase ~ 8 ℃ was found for PBS-injected mouse group, eliminating the possibility that the temperature rise in nanoparticle groups was caused by skin absorption of laser light. Moreover, laser irradiation-induced temperature elevation in FA-GNR@Pt group was 3~4 ℃ higher than that detected in GNR@Pt group when examined at four different time points post injection (Figure 5c). This could be most likely attributed to the increased intratumoral accumulation of FA-GNR@Pt nanoparticles than that of GNR@Pt counterpart.

Since GNR@Pt nanoparticles induced significant hyperthermia effect in vivo, we next evaluated the ability of GNR@Pt nanoparticles to ablate breast tumor in vivo. Nude mice bearing 4T1-Luc tumor were separated into three groups (n = 3) when the tumor volume reached 100 mm^3. The mice groupswere intravenously injected with PBS, GNR-PGA or GNR@Pt, respectively. Two hours post injection, the mice were then irradiated with 655 nm laser for 2 min at photo intensity of 1.0 W/cm^2, and the tumor growth was monitored using bioluminescence imaging (BLI) examination. As shown in Figure 5e&f, obvious increase of Luc activity was found in PBS group 7 days post laser treatment due to the fast growth of orthotopic 4T1 tumors. Luc expression in the GNR-PGA group was obviously suppressed by laser irradiation when examined 4 day post nanoparticle injection due to photothermal ablation of the cancer cells. The Luc activity recovered at the 7^{th} day post laser treatment, which could be most likely explained by tumor relapse due to incomplete elimination of the primary cancer cells. In significant contrast, Luc expression in GNR@Pt group was completely inhibited throughout the experimental period of 7 days, implying

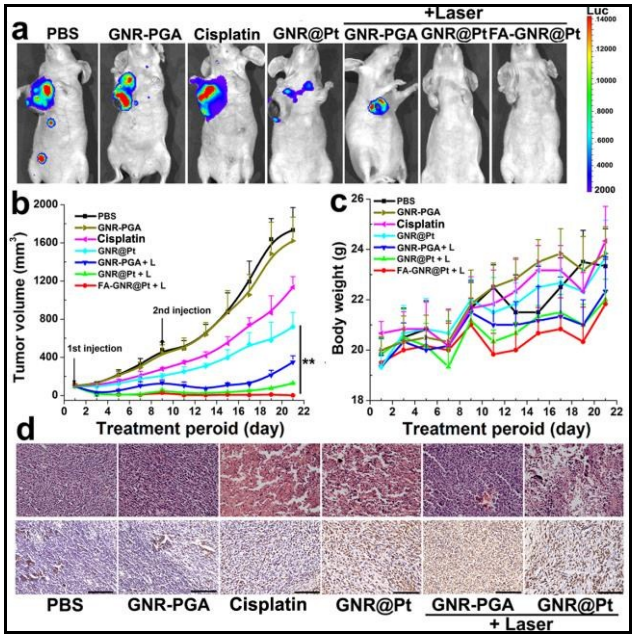

Fig. 6. Tumor growth inhibition assay of GNR@Pt nanoparticles administrated through tail vein injection. (a) Representative whole-body BLI images of 4T1-Luc tumor-bearing mice taken at the end of animal studies; (b) The tumor volume, and (c) Body weight change of tumor-bearing mice treated GNR@Pt nanoparticles and laser irradiation (n = 6, **p < 0.01); (d) Representative H&E (up), and Tunnel (bottom) stained microphotos (×200) of tumor sections (scale bar 200 μm).

successful ablation of the xenograft tumor. The superior therapeutic performance of GNR@Pt over that of GNR-PGA could be attributed to an addictive therapeutic effect between the hyperthermia effect of GNRs and chemotoxicity of cisplatin since GNR-PGA and GNR@Pt nanoparticles induced comparable temperature elevation upon laser illumination (Figure 5a&b).

As mentioned above, the growth and metastasis of solid tumors are closely related to the process of angiogenesis. To evaluate the ability of GNRs to ablate the tumor-associated blood vessels, the morphology of micro blood vessel was visualized by fluorescence angiography examination using a confocal laser endomicroscopy system with FITC-Dextran as a fluorescent probe. After injected with PBS and treated with 655 nm laser, strong green fluorescence assigned to FITC-Dextran was observed due to sufficient blood perfusion to the xenograft 4T1 tumor. The fluorescence pattern was not changed when injected with free cisplatin and irradiated with 655 nm laser. In contrast, more than 90% of the fluorescence signal was abolished in GNR-PGA plus laser group (Figure 5g). At the end of BLI examination, the tumoural microvessel density (MVD) of GNR-PGA, cisplatin or PBS-treated mouse group was semi-quantitatively examined by CD31 staining. As shown in Figure 5h, the MVD in the tumor tissue of GNR-PGA group was reduced by > 90%, along with the reduce of microvessel diameter from 25.5±6.0 μm to 4.7±1.5 μm, in significant contrast to that of PBS or cisplatin group. This strongly confirmed the successful elimination of tumor-associated blood vessels in GNR-PGA group.

Antitumor efficacy and biosafety of FA-GNR@Pt nanoparticles *in vivo*

We had showed that FA-GNR@Pt nanoparticles could deliver more cisplatin to the othtropic 4T1 tumor and induce higher temperature increase than GNR@Pt ones. We next asked whether FA-GNR@Pt nanoparticles could generate a better anti-tumor efficacy than GNR@Pt. To answer this question, nude mice bearing 4T1 tumors were randomly grouped into seven groups (n = 6) when the tumor volume reached 100 mm^3. The mice were then intravenously injected with cisplatin, GNR-PGA, GNR@Pt or FA-GNR@Pt at an equal cisplatin dose of 0.50 mg/kg or GNR dose of 6.9 mg/kg. The mouse group treated with 100 μL of PBS was set as a negative control. The tumor growth was examined by BLI examination at the end of animal study. As demonstrated in Figure 6a, spreading luciferase signal was found in PBS, PGA-GNR, cisplatin or GNR@Pt groups, confirming high proliferation activity of the primary tumor and metastasis of the cancer cells to the distant organs (i.e. the bone or lung). On the pronounced contrary, the luciferase expression was completely eradicated in the laser-irradiated GNR@Pt or FA-GNR@Pt group, implying laser irradiation significantly improved the therapeutic efficacy of GNR@Pt nanoparticles. The tumor growth was monitored by measuring the tumor volume during the treatment period. GNR@Pt group displayed much slower tumor growth rate than that found in the cisplatin-treated ones, which could be explained by the improved tumor distribution of cisplatin when delivered with GNRs. The slowest tumor growth rate was found in laser-treated FA-GNR@Pt group among all the mouse groups, followed by that of the irradiated GNR@Pt group (Figure 6b), suggesting a synergistic anti-tumor effect between laser irradiation and GNR@Pt. As an indicator of systemic toxicity, the body weight of all mouse groups were measured during the whole body weight of all mouse groups were measured during the whole treatment period. No obvious body weight loss was found in GNR-PGA group, indicating good biocompatibility of GNR-PGA nanoparticles in vivo. The laser treated mouse groups displayed much slower body weight increase rates than the group treated with other formulations (Figure 6c). This could be most likely explained by the lower tumor growth rates of these three groups.

To elucidate the possible mechanism for a combination of GNR@Pt treatment and laser irradiation to reduce tumor growth, the mice were sacrificed at the end of anti-tumor study. No identifiable malignant transformation area was found in FA-GNR@Pt group implying complete elimination of the orthotopic 4T1 tumor by FA-GNR@Pt nanoparticles performed combined PT and chemotherapy. The tumor organs in other animal groups were collected, fixed and sectioned for Hematoxylin and Eosin (H&E) staining assay. It was found that most of the cancer cells in the irradiated GNR@Pt group lost their membrane integrity, indicating notable necrosis of the cancer cells (Figure 6d, top panel), which might be caused by laser irradiation-induced hyperthermia effect. Significant cellular apoptosis were found by tunnel staining assay in the tumor section of cisplatin or GNR@Pt group, which increased further when the GNR@Pt injected group was treated with localized laser irradiation (Figure 6d, bottom panel). All these information suggested an addictive therapeutic effect between cisplatin-mediated chemotherapy and GNR-induced PT therapy in Laser+GNR@Pt group. In the meanwhile, the improved anticancer performance of FA-GNR@Pt over than that of GNR@Pt could be most likely

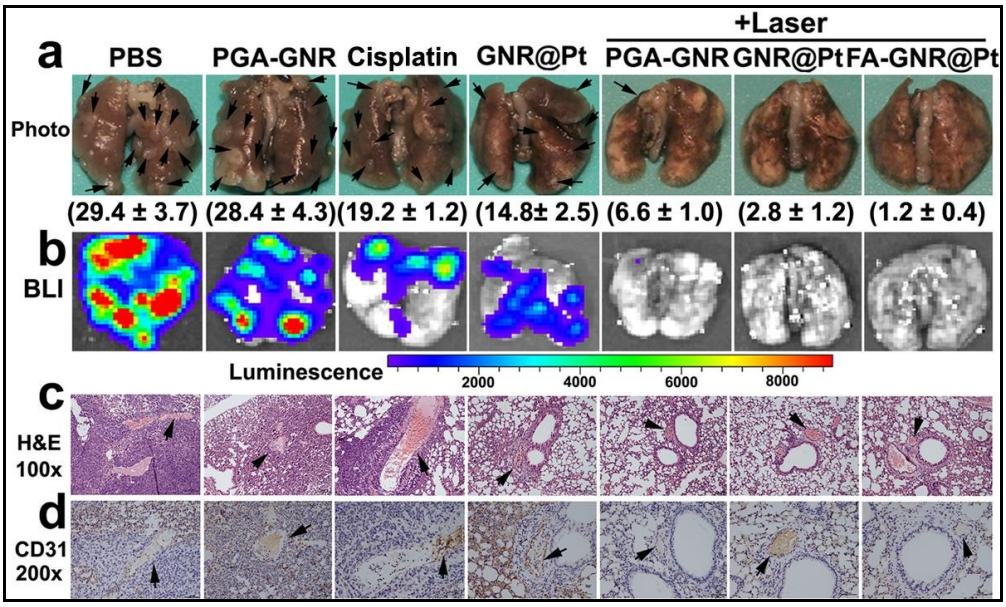

Fig. 7. GNR@Pt-mediated chemotherapy and photothermal ablation therapy prevented lung metastasis of orthotropic breast tumors. (a) The representative photographs, the average number of pulmonary metastasis nodules was shown in the bottom; (b) Corresponding BLI images of lungs from mice treated with different modalities; (c & d) Representative microphotos of the lung sections stained for (c) H&E (×100), and (d) CD31 (×200), respectively (the black arrow indicated the location of micro blood vessels in the lung) (scale bar 200 μm).

explained by the higher temperature elevation and the tumor targeted cisplatin distribution in the FA-GNR@Pt group (Figure 4c&d and Figure 5b&c).

We had demonstrated that intravenous injection of FA-GNR@Pt nanoparticles and laser irradiation could completely inhibit the growth of the primary tumor, we then wondered whether such a combination could simultaneously prevent the invasiveness and distant metastasis of the cancer cells? As shown in Figure 7a, inhibit the growth of the primary tumor, we then wondered whether such a combination could simultaneously prevent the invasiveness and distant metastasis of the cancer cells? As shown in Figure 7a, considerable metastasis nodules were found in the photographs of the lung tissue of PBS, PGA-GNR, cisplatin and GNR@Pt groups, confirming the strong metastasis potential of 4T1 cells. The lung metastasis of 4T1-Luc cells was also confirmed by BLI examination. Strong BLI signal assigned to the 4T1-Luc cells was found in the lung tissue of PBS, PGA-GNR, cisplatin and GNR@Pt groups. In outstanding contrast, no bioluminescence signal was found in the lung of the mouse groups treated with GNR-PGA, GNR@Pt or FA-GNR@Pt nanoparticles + laser illumination, implying complete lung metastasis inhibition of the cancer cells (Figure 7b).

To understand the possible mechanism of laser irradiation induced lung metastasis inhibition of 4T1 cells, the lung tissues of all moue groups were fixed and analysed for H&E staining assay. As expected, intensively stained metastasis nodules were found in the lung tissues of PBS, GNR-PGA, cisplatin or GNR@Pt group, and all the metastasis nodules were found surrounding the micro blood vessels as confirmed by CD31 staining assay (Figure 7 c&d). On the contrary, negligible metastasis nodules were found in the lungs of laser-treated groups Both the H&E and CD31 staining assays consistently suggested that transportation through bloodstream was the dominant pathway for metastasis of 4T1 cells from the primary tumor to the lung.[33] Thus, GNR@Pt nanoparticles in combination with laser irradiation could prevent the distant metastasis of the cancer cells by ablating of the tumor-associated blood vessels.

To evaluate the biosafety of GNR@Pt hybrid nanoparticles for systemic injection, the major organs (i.e. heart, liver, spleen, lung and kidney) were examined using a histological analysis. Although cisplatin-treatment induced obvious tubular atrophy and necrosis due to its severer nephrotoxicity, GNR@Pt and FA-GNR@Pt caused negligible damage in all major organs (Figure SI 17). Since GNR@Pt displayed obvious liver deposition, the influence of nanoparticle-injection on the liver function was examined by blood biochemical analysis. No significant difference was found between PBS and GNR@Pt groups regarding several factors including the serum levels of albumin, globulin, alkaline phosphatase, alanine aminotransferase, aspartate aminotransferase, total bilirubin level and total protein level (Table SI 1). Taken together, both the H&E and liver function data confirmed excellent biosafety of GNR@Pt nanoparticles.

The anti-tumor efficacy of GNR@Pt nanoparticles through intratumoral injection was also evaluated with the same regimen. A much lower GNRs or cisplatin dose than that used for systemic administration (i.e. 1.7 mg/kg of GNRs and 0.13 mg/kg of cisplatin respectively) was applied for intratumoral injection. As expected, higher temperature elevation (i.e. >30 ℃) was achieved by intratumroal injection than that induced by intravenous injection due to the increased GNRs concentration in the primary tumor (Figure SI 18). However, compared to intravenously injection, GNR@Pt administrated through intratumoral injection displayed lower efficiency to inhibit both the tumor growth and lung metastasis (Figure SI 19 & 20). This could be presumably caused by the lower permeability of the nanoparticles injected intratumorally than that of the nanoparticles administrated through tail vein injection. More importantly, the nanoparticles administrated systemically tend to accumulate in the perivascular area of the tumor organ due to

presence of the dense extracellular matrix.[34,35] The highly accumulated GNRs on the vasculature area in turn could induce significant temperature rise to destroy the endothelial cells, thus block the nutrient line for tumor growth and prevent escape of the cancer cells through blood flow.

Conclusions

In summary, the GNR@Pt hybrid nanoparticles displayed slightly negative surface charge and good colloidal stability in serum solution, thus allowing systemic administration. FA-modification significantly increased the tumoural accumulation of both GNRs and cisplatin by targeting the folate receptors of 4T1 breast cancer cells. The FA-GNR@Pt nanoparticles induced notable temperature rise both in vitro and in vivo upon 655 nm NIR laser irradiation. A combination of systemic administration of FA-GNR@Pt nanoparticles with localized laser irradiation was able to inhibit the proliferation and lung metastasis of the 4T1 breast tumor. The improved therapeutic efficacy of FA-GNR@Pt over that of GNR@Pt or GNRs alone could be attributed to FA-mediated tumor targeting effect, cisplatin-induced apoptosis of cancer cells, hyperthermia-caused necrosis of the cancer cells and ablation of the blood vessels. The platform described in this study could be a useful strategy to simultaneously inhibit the proliferation of the primary tumor and prevent its distant metastasis, which might provide novel insight for breast cancer therapy, specifically for treatment of TNBC with high potential of distant metastasis.

Acknowledgements

The authors thank Prof. Baohong Jiang and Dr. Yang Liu for assistance with the MVD measurement. Financial support from the National Basic Research Program of China (2013CB932704 and 2012CB932502), the National Natural Science Foundation of China (81373359, 21305047 and 81270047) and the Youth Innovation Promotion Association CAS is gratefully acknowledged.

Notes and references

1 C.L. Chaffer, R.A. Weinberg, *Science*, 2011, **331**, 1559.
2 A.J. Minn, G.P. Gupta, P.M. Siegel, P.D. Bos, W.P. Shu, D.D. Giri, et al. *Nature*, 2005, **436**, 518.
3 Carey L., Winer E., Viale G, Cameron D, Gianni L. *Nat. Rev. Clinic. Onco.*, 2010, **7**, 683.
4 S. Shen, X.J. Du, J. Liu, R. Sun, Y.H. Zhu, J. Wang, *J. Control. Release*, 2015, 208, 14.
5 S.E. Singletary, *Am Surgeon*, 2002, **184**, 383.
6 H. Yagata, Y. Kajiura, H. Yamauchi, *Breast Cancer*, 2011, **18**, 165.
7 K.D. Voduc, MCU. Cheang, S. Tyldesley, K. Gelmon, T.O. Nielsen, H. Kennecke, *J. Clinic. Onco.*, 2010, **28**, 1684.
8 LGM Daenen, JML Roodhart, M van Amersfoort, M Dehnad, W Roessingh, LH Ulfman, et al. *Cancer Res.*, 2011, **71**, 6976.
9 F. Fan, M.J. Gray, N.A. Dallas, A.D. Yang, G Van Buren, E. R. Camp, et al. *Mol Cancer Ther*, 2008, **7**, 3064.
10 J.M.L. Ebos, C.R. Lee, W. Cruz-Munoz, G.A. Bjarnason, J.G. Christensen, R.S. Kerbel. *Cancer Cell*, 2009, **15**, 232.
11 I.S.Vala, L.R. Martins, N. Imaizumi, R.J. Nunes, J. Rino, F. Kuonen, et al. *PloS One*, 2010, **5**, e11222.
12 D. Hanahan, R.A. Weinberg, *Cell*, 2011, **144**, 646.
13 R.K. Jain, *Science*, 2005, **307**, 58.
14 M. Martin, *Current Opin Onco*, 2011, **23** Suppl:S1.
15 H.J. Lenz, *Oncology*, 2005, **19**, 17.
16 A.M. Gobin, M.H. Lee, N.J. Halas, W.D. James, R.A. Drezek, J.L. West. *Nano Letters*, 2007, **7**, 1929.
17 L. Au, D. Zheng, F. Zhou, Z.Y. Li, X. Li, Y. Xia, *ACS Nano*, 2008, **2**, 1645.
18 J.G. Piao, L.M. Wang, F. Gao, Y.Z. You, Y.J. Xiong, L.H. Yang. *ACS Nano*, 2014, **8**, 10414.
19 B. Jang, J.Y. Park, C.H. Tung, I.H. Kim, Y. Choi, *ACS Nano*, 2011, **5**, 1086.
20 C. Liang, S. Diao, C. Wang, H. Gong, T. Liu, G. Hong, et al. *Adv Mater*, 2014, **26**, 5646.
21 Z. Xiao, C. Ji, J. Shi, E.M. Pridgen, J. Frieder, J. Wu, et al. *Angew Chem Int Ed*, 2012, **51**, 11853.
22 S. Su, Y. Tian, Y. Li, Y. Ding, T. Ji, M. Wu, et al. *ACS Nano*, 2015,**9**,1367.
23 X.H. Huang, I.H. El-Sayed, W. Qian, M.A. El-Sayed. *J Am. Chem Soc.*, 2006, 1**28**, 2115.
24 C. Kinnear, D. Burnand, M.J.D. Clift, A.F.M. Kilbinger, B. Rothen-Rutishauser, A. Petri-Fink. *Angew. Chem. Int. Ed.*, 2014, **53**, 12613.
25 F.M. Mickler, Y. Vachutinsky, M. Oba, K. Miyata, N. Nishiyama, K. Kataoka, et al. *J Control Release*, 2011, **150**, 364.
26 N. Nishiyama, S. Okazaki, H. Cabral, M. Miyamoto, Y. Kato, Y. Sugiyama, et al. *Cancer Res*, 2003, **63**, 8977.
27 K. Osada, H. Cabral, Y. Mochida, S. Lee, K. Nagata, T. Matsuura, et al. *J. Am. Chem. Soc.*, 2012, **134**, 13172.
28 H. Yu, Z. Tang, D. Zhang, W. Song, Y. Zhang, Y. Yang, et al. *J Control Release*, 2014, **205**, 89.
29 H. Yu, Y. Nie, C. Dohmen, Y. Li, E. Wagner. *Biomacromolecules*, 2011, **12**, 2039.
30 K. de Bruin, N. Ruthardt, K. von Gersdorff, R. Bausinger. E.Wagner, M. Ogris, et al. *Mol. Ther.*, 2007, **15**, 1297.
31 H.J. Yu, J.Q. Wang, X.T. Shi, D.V. Louzguine-Luzgin, H.K. Wu, J.H. Perepezko. *Adv. Funct. Mater*, 2013, **23**, 4793.
32 P. Yu, H. Yu, C. Guo, Z. Cui, X. Chen, Q. Yin, et al. *Acta Biomater*, 2015, **14**, 115.
33 P. S. Steeg, *Nat. Rev. Cancer*, 2003, **3**, 55.
34 R. Tong, H.H. Chiang, D.S. Kohane, *Proc. Natl. Acad. Sci. USA*,2013, **110**, 19048.
35 A.J. Gormley, N. Larson, S. Sadekar, R. Robinson, A. Ray, H. Ghandehari, *Nano Today*, 2012, **7**, 158.